AMERICAN SOCIETY FOR MICROBIOLOGY | Journal of Virology®

VIRUS-CELL INTERACTIONS

Loss of the Human Cytomegalovirus US16 Protein Abrogates Virus Entry into Endothelial and Epithelial Cells by Reducing the Virion Content of the Pentamer

Anna Luganini,[a] Noemi Cavaletto,[a] Stefania Raimondo,[b] Stefano Geuna,[b] Giorgio Gribaudo[a]

Department of Life Sciences and Systems Biology,[a] and Department of Clinical and Biological Sciences,[b] University of Torino, Turin, Italy

ABSTRACT The human cytomegalovirus (HCMV) US12 gene family encodes a group of predicted seven-transmembrane proteins whose functions have yet to be established. While inactivation of individual US12 members in laboratory strains of HCMV does not affect viral replication in fibroblasts, disruption of the US16 gene in the low-passage-number TR strain prevents viral growth in endothelial and epithelial cells. In these cells, the US16-null viruses fail to express immediate early (IE), early (E), and late (L) viral proteins due to a defect which occurs prior to IE gene expression. Here, we show that this defective phenotype is a direct consequence of deficiencies in the entry of US16-null viruses in these cell types due to an impact on the gH/gL/UL128/UL130/UL131A (pentamer) complex. Indeed, viral particles released from fibroblasts infected with US16-null viruses were defective for the pentamer, thus preventing entry during infections of endothelial and epithelial cells. A link between pUS16 and the pentamer was further supported by the colocalization of pUS16 and pentamer proteins within the cytoplasmic viral assembly compartment (cVAC) of infected fibroblasts. Deletion of the C-terminal tail of pUS16 reproduced the defective growth phenotype and alteration of virion composition as US16-null viruses. However, the pentamer assembly and trafficking to the cVAC were not affected by the lack of the C terminus of pUS16. Coimmunoprecipitation results then indicated that US16 interacts with pUL130 but not with the mature pentamer or gH/gL/gO. Together, these results suggest that pUS16 contributes to the tropism of HCMV by influencing the content of the pentamer into virions.

IMPORTANCE Human cytomegalovirus (HCMV) is major pathogen in newborns and immunocompromised individuals. A hallmark of HCMV pathogenesis is its ability to productively replicate in an exceptionally broad range of target cells. The virus infects a variety of cell types by exploiting different forms of the envelope glycoprotein gH/gL hetero-oligomers, which allow entry into many cell types through different pathways. For example, incorporation of the pentameric gH/gL/UL128/UL130/UL131A complex into virions is a prerequisite for infection of endothelial and epithelial cells. Here, we show that the absence of US16, a thus far uncharacterized HCMV multitransmembrane protein, abrogates virus entry into endothelial and epithelial cells and that this defect is due to the lack of adequate amounts of the pentameric complex in extracellular viral particles. Our study suggests pUS16 as a novel viral regulatory protein important for shaping virion composition in a manner that influences HCMV cell tropism.

KEYWORDS human cytomegalovirus, pentamer, UL130, US12 gene family, US16 protein, endothelial cells, epithelial cells, virus entry

Received 6 February 2017 **Accepted** 14 March 2017

Accepted manuscript posted online 22 March 2017

Citation Luganini A, Cavaletto N, Raimondo S, Geuna S, Gribaudo G. 2017. Loss of the human cytomegalovirus US16 protein abrogates virus entry into endothelial and epithelial cells by reducing the virion content of the pentamer. J Virol 91:e00205-17. https://doi.org/10.1128/JVI.00205-17.

Editor Klaus Frueh, Oregon Health and Science University

Address correspondence to Giorgio Gribaudo, giorgio.gribaudo@unito.it.

Human cytomegalovirus (HCMV) is a major opportunistic pathogen in individuals with acquired or developmental deficiencies in innate and adaptive immunity. Indeed, HCMV is the leading viral cause of congenital disease and a common cause of morbidity and mortality in AIDS patients and organ transplant recipients (1–3). The pathogenesis of HCMV diseases is greatly influenced by the exceptionally broad range of target cells into which the virus can enter and then productively replicate. Indeed, among the HCMV-susceptible cell types, the predominant targets for massive productive viral replication in the natural host are fibroblasts of connective tissues, epithelial cells of mucosal tissue and glands, smooth muscle cells in the gastrointestinal tract, and vascular endothelial cells (3–6).

In order to infect such a remarkable range of different cell types successfully, each type with its own unique biochemical characteristics, HCMV has evolved the ability to exploit multiple and ubiquitous cell receptors, and it has developed a generous glycoprotein coding capacity such that it can form different and, in some cases, modular envelope complexes that mediate interactions with different cellular receptors (6, 7). Prototypical examples of such a modular virion complex are the two glycoprotein gH/gL-containing multimeric complexes that regulate virus cell tropism through interaction with cell-type-specific receptors and that trigger virus entry via direct interaction with the fusion protein gB (6–8). In fact, in HCMV virions, gH/gL can be either part of the gH/gL/gO trimer or part of the pentameric complex (pentamer) formed between gH/gL and the UL128, UL130, and UL131A proteins (8). HCMV entry into fibroblasts requires gH/gL/gO and arises through direct fusion with the cell plasma membrane while entry into endothelial and epithelial cells, dendritic cells, and monocytes involves macropinocytosis or endocytosis and low-pH-dependent fusion with endosomes and requires the pentamer (6–8). Thus, the proteins UL128 to UL131 represent major viral determinants of endothelial and epithelial cell tropism since mutation or deletion of any of the corresponding genes impairs HCMV entry into these cell types (5–7).

However, the results of genome-wide and functional studies point toward the existence of additional HCMV genes required for the successful completion of the viral infection cycle in endothelial and epithelial cells (9–11). In this regard, we observed that inactivation of the US16 gene in the low-passage-number TR strain severely impaired virus replication in different types of endothelial and epithelial cells (12) and in dendritic cells (A. Luganini and G. Gribaudo, unpublished data). US16 belongs to the US12 gene family that includes a set of 10 contiguous genes arranged in tandem (US12 to US21) in the unique short (US) region of the HCMV genome (11, 13). This gene family has been identified only in cytomegaloviruses specific to higher primates, such as rhesus CMV (RhCMV) and chimpanzee CMV (CCMV) (13). The identification of putative seven-transmembrane hydrophobic domains in each of the US12 open reading frames (ORFs) would predict a common structural framework that associates these proteins with cellular membranes (13). Deletion of individual family members or even the entire US12 locus from the genome of HCMV laboratory strains did not influence viral replication in fibroblasts (9, 10). Consequently, it has been hypothesized that the US12 genes may exert regulatory roles in the infection of specific cell types and/or under different physiological conditions *in vivo* (13). Their pronounced conservation among different HCMV strains supports their importance and requirement during HCMV infection in the host (11). Nonetheless, the expression, localization, and functions of most of the US12 proteins remain to be defined.

In our previous report, we observed that US16-mutant viruses failed to express representative immediate early (IE), early (E), and late (L) viral proteins and to deliver the tegument protein pp65 and incoming viral DNA to nuclei in infected endothelial and epithelial cells, thus suggesting that the US16 gene regulates, in a cell-type-specific manner, a phase of the HCMV replication cycle occurring after virion attachment but prior to the release of the viral genome into the nucleus (12). Nevertheless, a direct role of US16 in viral entry into endothelial and epithelial cells was unlikely as no US16 protein could be detected in extracellular virus particles purified from culture supernatants of HCMV-infected fibroblasts (12). This observation led us to hypothesize that

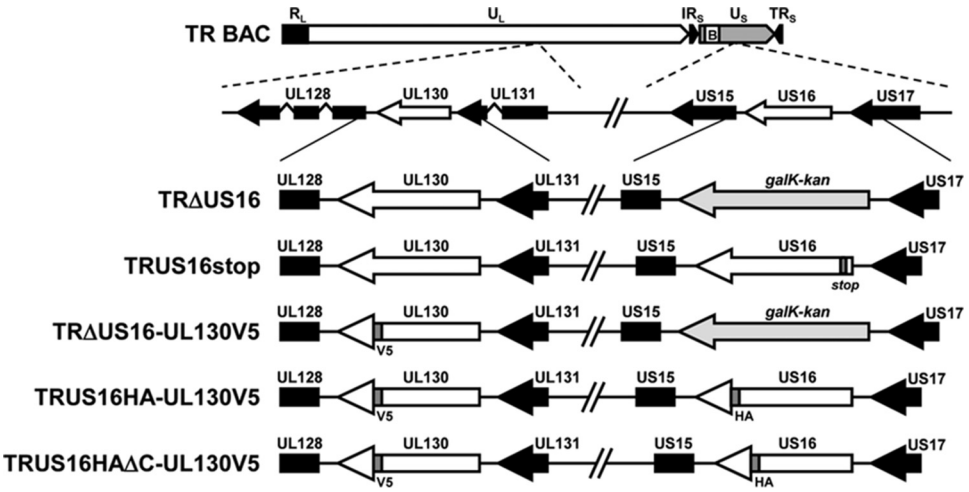

FIG 1 A schematic representation of the HCMV US16 and UL130 gene regions and the modifications introduced into the ORFs. In TRΔUS16, the US16 ORF was replaced with a cassette containing the *galK-kan* genes. In TRUS16stop, a single nucleotide change was introduced into codons 9, 10, and 11 of the US16 ORF. These changes created a stop codon in the 10th codon (12). The TRUS16HA-UL130V5 was generated from TRUS16HA-ΔUL130 BAC by reintroducing the UL130 ORF fused with the coding sequence for a V5 epitope tag at its C terminus. In the TRΔUS16-UL130V5, the US16 ORF was replaced with the *galK-kan* cassette. In TRUS16HAΔC-UL130V5, the *galK-kan* gene of TRΔUS16-UL130V5 BAC was replaced with a C-terminal truncation of the US16 ORF lacking 34 amino acids (from 276 to 309) fused in frame with an HA epitope tag at its C terminus. Recombinant BACs were examined for the desired mutations by PCR and sequencing. U_L, unique long region; IR_S, short inverted repeat; R_L, long inverted repeat; TR_S, short terminal repeat.

pUS16 could modulate some entry-related events even though it is not incorporated into virions.

The present study addresses this hypothesis by investigating the role of US16 protein in the entry process of an endothelio- and epitheliotropic HCMV strain. Specifically, inactivation of the US16 ORF impaired entry of US16-null viruses into endothelial and epithelial cells, and this defect correlated with the absence of representative pentamer proteins in purified extracellular virions produced by a US16-null virus. However, even in the absence of functional pUS16, neither the trafficking of the pentamer to the cytoplasmic viral assembly compartment (cVAC) nor cVAC formation was altered, thus suggesting that pUS16 contributes to determine the final glycoprotein composition of the envelope of HCMV particles in a manner that influences the virus cell tropism.

RESULTS

Inactivation of the US16 gene abrogates entry of HCMV into endothelial and epithelial cells. To investigate whether entry into endothelial and epithelial cells was defective in US16-mutant viruses, ARPE-19 cells, an *in vitro* epithelial cell model, were infected with wild-type (wt) TR (TRwt), TRΔUS16, or TRUS16stop (Fig. 1) or with the AD169 or Towne strain, two HCMV strains defective for entry into endothelial and epithelial cells (5–7). Cells were then briefly treated with 44% polyethylene glycol (PEG), reported to overcome defects in virus entry in the entry-defective UL128-to-UL150 deletion mutant from strain TR when the virus is adsorbed to the cell surface of epithelial cells (14). Infection rates were assessed at 24 h postinfection (p.i.) by indirect immunofluorescence detection of IEA (IE1 plus IE2) proteins. As shown in Fig. 2A (left panel), the PEG treatment greatly increased the percentage of epithelial cells infected with TRΔUS16 or TRUS16stop to levels almost similar to the level observed with TRwt (on average, 8% was observed for TRΔUS16, 12% for TRUS16stop, and 13% for TRwt). Quantitative microscopic analysis showed more than a 40-fold increase in the frequency of IEA detection following the treatment of TRΔUS16- or TRUS16stop-infected cells with PEG (Fig. 2A, right panel), thus indicating that US16-deficient viruses, like AD169 and Towne, were defective for entry into epithelial cells.

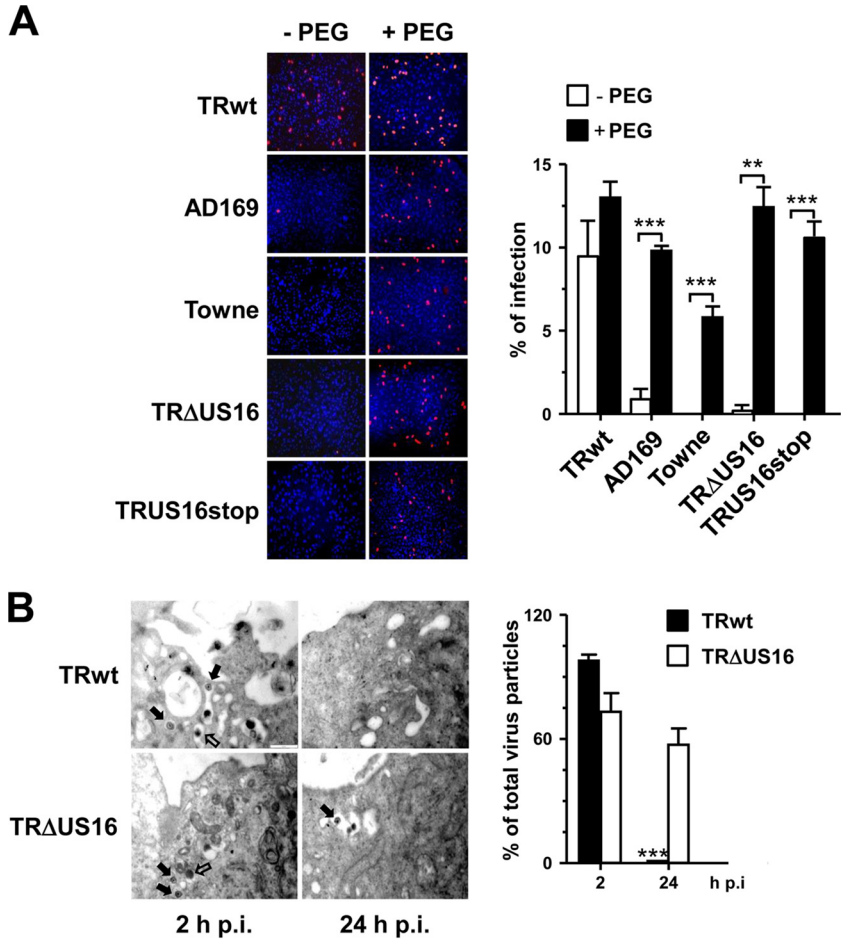

FIG 2 The US16 gene is required for entry into endothelial and epithelial cells. (A) Effect of PEG on the infection rate of US16-mutant viruses in epithelial cells. ARPE-19 cells were infected with TRwt, AD169, Towne, TRΔUS16, or TRUS16stop (MOI of 0.1 PFU/cell), centrifuged at 2,000 rpm for 30 min, and then incubated at 37°C for 2 h. Infected cells were then treated with either PBS or 44% PEG for 60 s. At 24 h p.i., cells were fixed, permeabilized, and stained with an anti-IEA (IE1+IE2) MAb. Immunofluorescence experiments were repeated three times, and representative microscope fields are shown (left). Images from cells infected with AD169 or TRΔUS16 and then left untreated were purposely chosen to include some positive nuclei to show virus addition since random fields were generally negative for IEA staining. Magnification, ×10. The average percentages of the ratio of IEA-positive nuclei to DAPI-stained nuclei for 20 different microscope fields are shown (right). Data shown are the means ± SD. **, $P < 0.001$; ***, $P < 0.0001$, for results with the indicated viruses versus those with the calibrator sample (cells infected with TRwt, AD169, Towne, TRΔUS16, or TRUS16stop, and then not treated with PEG). (B) US16-deficient virus fails to release viral particles from endocytic vesicles in endothelial cells. HMVECs were infected with TRwt or TRΔUS16 (MOI of 30 PFU/cell) at 4°C for 2 h. Infected cells were then incubated at 37°C and, at the indicated times, fixed, embedded, and sectioned for transmission electron microscopy. Representative micrographs of three independent experiments are shown (left). Filled black arrows indicate mature virions; open arrows show dense bodies. Magnification, ×40,000. Scale bar (top left), 0.5 μm. The average percentages of virus particles counted inside endosomes are shown (right). Eight fields were analyzed for each of 10 cells evaluated for each virus at 2 and 24 h p.i. Data shown are the means ± SD. ***, $P < 0.0001$, for results with the indicated viruses versus those with the calibrator sample (2 h p.i. versus 24 h p.i.).

To support this observation further and to investigate the fate of viral particles generated by a US16-deficient virus, we performed ultrastructural analysis by transmission electron microscopy in the other cell type tested, i.e., endothelial cells. To this end, human dermal microvascular endothelial cells (HMVECs) were infected with purified TRwt or TRΔUS16 virus particles at a multiplicity of infection (MOI) of 30 and then processed for electron microscopy at 2 and 24 h p.i. As shown in Fig. 2B, at 2 h p.i., both viruses were internalized, and virions and dense bodies were found to accumulate in vacuoles within the cytoplasm of infected HMVECs. However, at 24 h p.i., more than

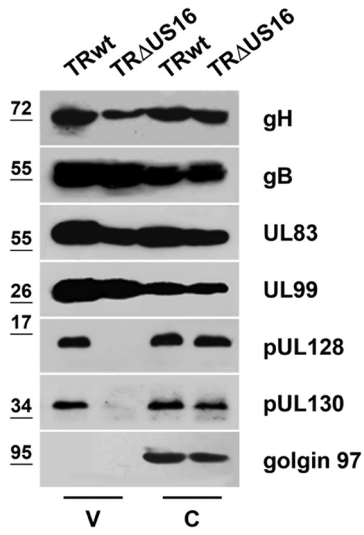

FIG 3 Inactivation of the US16 gene impairs incorporation of pentamer proteins into viral particles. TRwt and TRΔUS16 extracellular virion particles were purified from culture supernatants of infected HFFs by centrifugation through 20% sorbitol cushions. Protein extracts prepared from virions (V) or infected cells (C) were then fractionated through SDS-PAGE gels and analyzed by immunoblotting with mouse MAbs specific for gH, gB, UL83, UL99, UL128, or UL130. Immunodetection of golgin-97, a marker for the *trans*-Golgi network, was performed as a control for cell protein contamination. Molecular mass markers are indicated for each panel.

70% of the TRΔUS16 virions present in cells at early times of infection could still be detected within cytoplasmic vesicles while TRwt particles were no longer observed in the cytoplasm of infected HMVECs (Fig. 2B, right panel); this observation is consistent with the accepted model of TR entry into endothelial cells, which involves macropinocytosis or endocytosis and the release of nucleocapsids from the vesicles following the low-pH-dependent fusion with endosomes (7, 8, 14, 15).

Taken together, these results suggest that an intact US16 ORF is required in the producer cells (e.g., fibroblasts) to generate viral particles capable of entry into both endothelial and epithelial cells.

HCMV virions produced by US16-null virus are defective for pentamer proteins. The presence of an adequate content of the pentamer in virions is a prerequisite for successful infection of endothelial and epithelial cells (6–8). Therefore, to test whether the defective phenotype of genotypically US16-negative viruses was associated with a change of the pentamer abundance, extracellular virus particles harvested from supernatants of human foreskin fibroblast (HFF) cultures infected with TRwt or TRΔUS16 were purified by ultracentrifugation (12), and their protein compositions were compared by immunoblot analysis with the protein extracts prepared from TRwt- and TRΔUS16-infected HFFs. The presence of representative pentamer proteins, such as pUL128 and pUL130, was assessed along with that of UL99 (pp28), UL83 (pp65), gB, and gH as a control for tegument and envelope glycoproteins. Golgin-97, a protein associated with the cytoplasmic face of the *trans*-Golgi network (TGN) and observed in the cVAC of HCMV-infected fibroblasts (16), was analyzed to control for cell membrane contamination and was not detected in the purified extracellular particles (Fig. 3). The relative abundances of UL99, UL83, and gB were not significantly different between virions produced by TRwt and TRΔUS16, while a reduced gH content was observed in extracellular virus particles released from cells infected with the US16-deficient virus (Fig. 3). However, the most substantial differences were measured for pUL128 and pUL130. As expected, these two pentamer proteins were observed in TRwt particles and in the corresponding infected cell extracts and in extracts prepared from TRΔUS16-infected HFFs (Fig. 3). In contrast, the pUL128 and pUL130 contents in TRΔUS16 virions were reduced to virtually undetectable levels in comparison to the levels seen in TRwt;

this suggested that the defective entry of US16-deficient viruses was due to the absence of adequate levels of the pentamer. Moreover, the fact that the levels of pUL128 and pUL130 observed in TRΔUS16-infected HFFs were similar to those in TRwt-infected cells (Fig. 3) indicated that the lack of the US16 gene did not affect their expression proteins but, rather, the subsequent stages of pentamer maturation, such as its formation or trafficking and/or incorporation into mature viral particles.

pUS16 and representative pentamer proteins colocalize within the cVAC of producing cells. To investigate in more depth the relationship between pUS16 and the pentamer pathway in the context of the viral replication cycle, we generated two further derivatives of TRwt. In TRUS16HA-UL130V5 (Fig. 1), the US16 ORF is expressed as a fusion protein with a hemagglutinin (HA) epitope tag sequence at its carboxyl terminus, and the UL130 ORF is expressed as a fusion protein with a V5 epitope tag at its carboxyl terminus. In the TRΔUS16-UL130V5 derivative (Fig. 1), the US16 coding region of the TRUS16HA-UL130V5 bacterial artificial chromosome (BAC) was replaced with a *galK-kan* cassette. The expression levels of tagged pUS16HA and pUL130V5 were examined by immunoblot analysis of total cell protein extracts prepared at different times p.i. from HFFs infected with TRUS16HA-UL130V5 or with TRΔUS16-UL130V5 (Fig. 4A). pUS16HA and pUL130V5 were both first detected at 48 h p.i. and persisted until 96 h p.i. As expected, the expression of pUS16HA was not observed in cells infected with the US16-null TRΔUS16-UL130V5 virus. The replication kinetics of TRUS16HA-UL130V5 and TRΔUS16-UL130V5 showed no apparent differences on HFFs (data not shown), while those of TRUS16HA-UL130V5 in HMVECs and ARPE-19 cells (Fig. 4B) were similar to those of TRwt. In contrast, the disruption of the US16 coding region in TRΔUS16-UL130V5 caused, as expected, a severe growth defect in both HMVECs and ARPE-19 cells (Fig. 4B), as previously seen in TRΔUS16 and TRUS16stop viruses (12). Altogether, these results validate the use of TRUS16HA-UL130V5 and TRΔUS16-UL130V5 viruses as appropriate initial tools for investigating the intracellular location of pUS16HA and pUL130V5 in infected cells by means of immunofluorescence.

Since HCMV infection induces a profound reorganization of several components of the cellular secretory machinery that rearrange during late stages of infection into the cytoplasmic virion assembly complex (VAC) (17–20), we wanted to investigate whether pUS16 accumulates within the VAC. To this end, in HCMV-infected HFFs we examined the localization of pUS16 and three cellular organelle markers, GM130 (a *cis*-medial Golgi complex marker), EEA1 (an early endosomal marker), and CD63 (a late endosome marker), that are all reorganized by HCMV infection toward the periphery (pUS16) and the center (the organelle markers) of the cVAC (17, 18). In HFFs infected with TRUS16HA-UL130V5 for 120 h p.i., by which time the cVAC is fully formed (17, 18), pUS16HA showed a distinctive ring-like cytoplasmic staining pattern with remarkable overlap of the GM130 pattern (Fig. 5A). The ring-like structure revealed by staining with the anti-GM130 monoclonal antibody (MAb) is the consequence of HCMV-induced remodeling of GM130-containing Golgi stacks within the cytoplasm of uninfected cells and corresponds to the peripheral cylinder structure of the cVAC (17, 18). When TRUS16HA-UL130V5-infected HFFs were immunostained for pUS16HA and EEA1 or for CD63, the pUS16HA-positive ring-like cytoplasmic structure partially overlapped the structures of the other two markers in the periphery of the cVAC (Fig. 5A). Moreover, pUS16-HA partially colocalized within the periphery of cVAC with gH and gB, two viral glycoproteins that are known to accumulate in the cVAC (19) and that showed a more concentrated staining pattern in the central part of the cVAC (Fig. 5A).

The intracellular localization of pUS16HA relative to that of pUL130V5 was then investigated at time points spanning the entire HCMV replication cycle in TRUS16HA-UL130V5-infected HFFs (Fig. 5B). Consistent with the immunoblot analysis (Fig. 4A), pUS16 staining was first detectable at 48 h p.i. and, similar to staining of pUL130V5, displayed a diffuse pattern throughout the cytoplasm of infected cells up to 72 h p.i. (Fig. 5B). As infection progressed, starting from 96 h p.i., the intracellular localizations of both pUS16HA and pUL130V5 changed as they began to display a staining pattern similar to that of GM130 in infected cells, with the characteristic ring-like shape, which

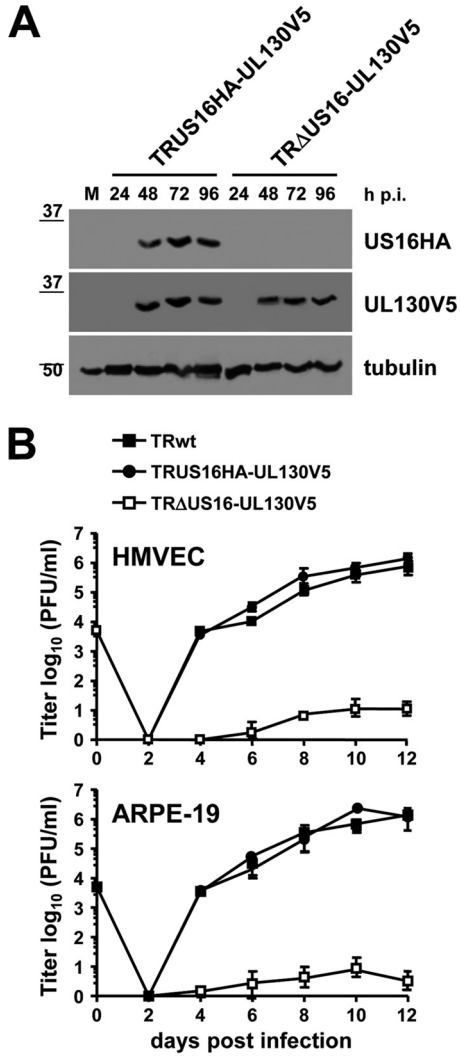

FIG 4 Characteristics of TRUS16HA-UL130V5 and TRΔUS16-UL130V5 viruses. (A) Kinetics of pUS16HA and pUL130V5 protein expression. HFFs were mock infected (lane M) or infected with TRUS16HA-UL130V5 or TRΔUS16-UL130V5 (MOI of 1 PFU/cell). At the indicated times p.i., total protein cell extracts were prepared, fractionated by SDS-PAGE, and analyzed by immunoblotting with anti-HA or anti-V5 MAb. The immunodetection of tubulin with an MAb was performed as an internal control. (B) Replication of TRUS16HA-UL130V5 and TRΔUS16-UL130V5 in endothelial and epithelial cells. HMVECs and ARPE-19 cells were infected with the parental TRwt, TRUS16HA-UL130V5, or TRΔUS16-UL130V5 (MOI of 0.1 PFU/cell). The extent of virus replication was determined by plaque assay in HFFs. The data shown are the averages of three experiments ± SD.

became increasingly evident at 120 h p.i. when most of the pUS16HA and pUL130V5 staining overlapped within the ring-like structure (Fig. 5B), thus indicating that in the context of infection, the two proteins colocalized in the periphery of the cVAC. Multicell assessment of the Pearson's coefficient of colocalization (21) confirmed that pUS16HA and pUL130V5 have higher levels of colocalization with gB and gH than pUS16HA (Fig. 5C).

This last observation led us to investigate the membrane topology of pUS16 relative to the intraluminal localization of pUL130 (22). The potential transmembrane domain (TMD) regions of pUS16 were predicted using five different algorithms: Phyre, version 2.0 (23), MEMSAT3 (24), MEMSAT_SVM (24), TopPred, version 0.01 (25), and TMHMM, version 2.0 (26). All algorithms were consistent in predicting a cytoplasmic N terminus. However, two different topology profiles were proposed: one with six TMDs (TMHMM, version 2.0) and another with seven TMDs (Phyre, version 2.0, MEMSAT3, MEMSAT_

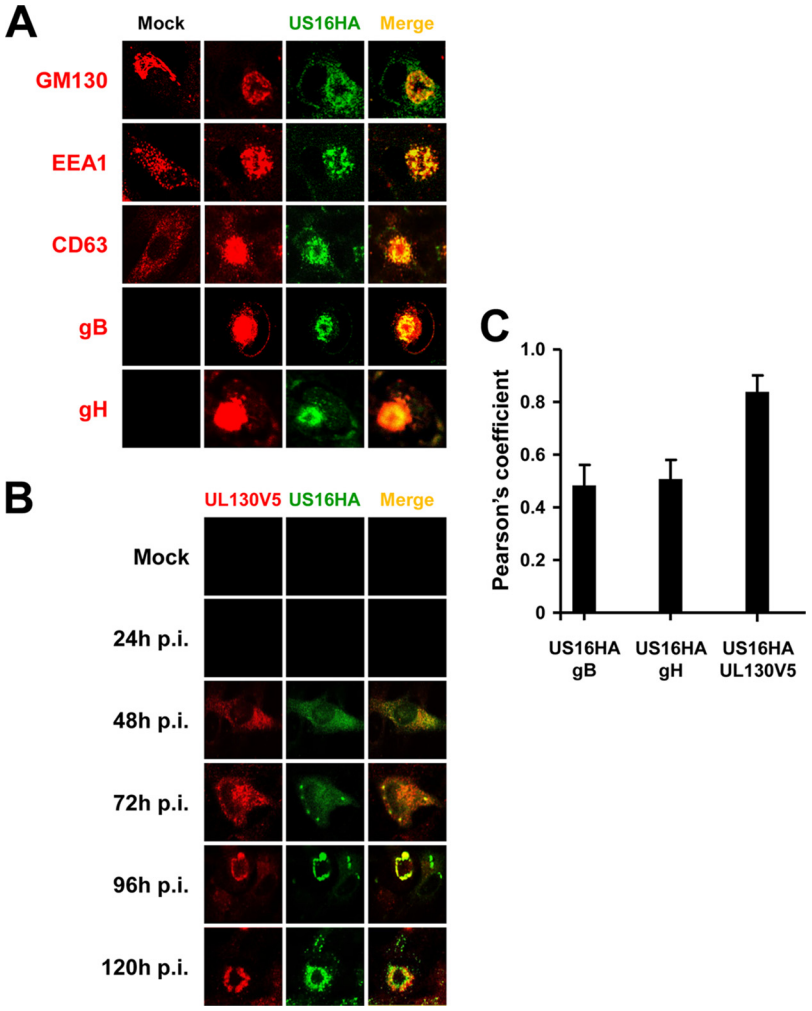

FIG 5 pUS16 accumulates in the cVAC of infected cells and colocalizes with pUL130 within the peripheral zone. (A) pUS16HA localizes within the cVAC. HFFs were infected with TRUS16HA-UL130V5 (MOI of 1 PFU/cell) or mock infected. At 120 h p.i., the cells were fixed, permeabilized, and stained for pUS16HA (green) and for GM130 (Golgi marker), EEA1 (early endosomal marker), CD63 (late endosomal marker), gB, and gH (red). (B) pUS16HA colocalizes with pUL130V5 in the periphery of cVAC at late times during infection. HFFs were infected with TRUS16HA-UL130V5 (MOI of 1 PFU/cell) or mock infected, and at various times p.i. cells were fixed, permeabilized, and immunostained with an anti-HA and anti-V5 MAbs. Immunofluorescence experiments were repeated three times; representative images visualized by confocal microscopy are presented. Magnification, ×60. (C) Colocalization coefficients for pairs of viral markers. Pearson's correlation for colocalization of signals between pUS16HA and gB, gH, or pUL130 was determined in confocal microscopy images collected from experiments included in panels A and B. Ten randomly chosen fields were evaluated for each pair of makers. The data shown are the averages of three independent experiments ± SD.

SVM, and TopPred, version 0.01). To address this discrepancy and to determine whether the C terminus of pUS16HA was cytosolic or luminal, an epitope accessibility assay was adopted after the selective permeabilization of HFFs with either 20 μM digitonin, to permeabilize the plasma membrane only (leaving internal membranes, such as the Golgi apparatus and the endoplasmic reticulum [ER], intact), or with 0.1% Triton X-100, which allows complete permeabilization and antibody accessibility to epitope tags regardless of their orientation within any membrane (27). The cellular markers GM130 (a protein that is tightly bound to the cytosolic side of *cis*-Golgi membranes) (28) and calreticulin (a luminal ER protein) (29), along with UL83 (pp65) (a tegument protein that accumulates in the cytoplasm late in infection) (30) and gB and gH (luminal viral glycoproteins), were used to validate the selective permeabilization assay for detection of membrane-associated cytosolic or luminally oriented epitopes (Fig. 6). The orienta-

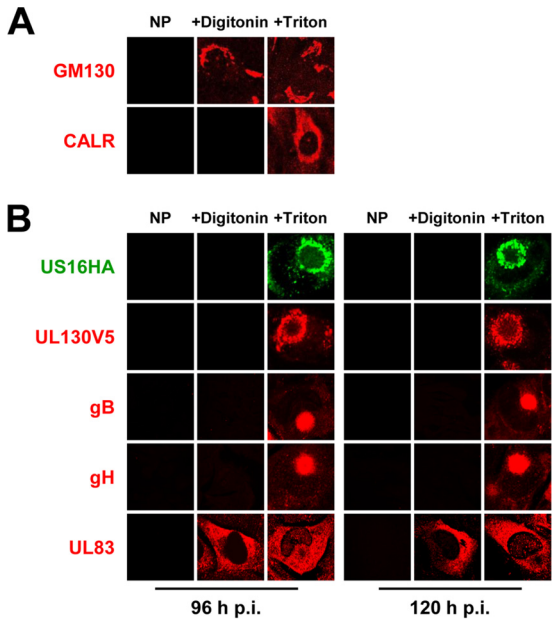

FIG 6 C-terminal topology of pUS16 and pUL130. HFFs were infected with TRUS16HA-UL130V5 (MOI of 1 PFU/cell), and at 96 and 120 h p.i. cells were selectively or completely permeabilized using digitonin (+Digitonin) or Triton X-100 (+Triton) or not permeabilized (NP). The pUS16 and pUL130 C-terminal tags were then immunostained with MAbs to HA and V5, respectively. GM130 and calreticulin (CALR) staining was used as a control of mock-infected cells (A). gB, gH, and UL83 (pp65) staining was used to control for selective permeabilization of infected cells (B). Images are representative of three independent experiments. Magnification, ×60.

tion of the C terminus of pUS16 relative to that of pUL130 was thus determined by staining TRUS16HA-UL130V5-infected HFFs with both anti-V5 and anti-HA MAbs. However, only Triton X-100 treatment allowed immunostaining of the C terminus of pUS16 (Fig. 6B), thus demonstrating that it was located on the luminal side of a cVAC membrane, most likely a Golgi complex-derived compartment as suggested by the overlap of the pUS16 and GM130 staining in the periphery of the cVAC (Fig. 5); these results argue in support of the predicted seven-TMD topology of pUS16. Moreover, the staining of pUL130 was observed only after Triton X-100 permeabilization, as expected from the accepted model of the pentamer structure in which gL, pUL128, pUL130, and pUL131A are all bound to the intraluminal/extracellular portion of gH (6–8).

Taken together, the results shown in this section indicate that pUS16 is a seven-TMD protein that colocalizes late in infection with pUL130 within Golgi complex-derived vesicles of the cVAC.

The C-terminal tail of pUS16 is essential for efficient HCMV replication in endothelial and epithelial cells. To investigate the importance of the pUS16 C-terminal tail in conferring the virus tropism for endothelial and epithelial cells, we generated a derivative of TRUS16HA-UL130V5 BAC, the TRUS16HAΔC-UL130V5 BAC, in which the US16HA gene is replaced with an HA-tagged C-terminal truncation variant lacking the last 34 amino acids (from 276 to 309) of the wt US16 ORF (Fig. 1). The expression levels of pUS16HA and pUS16HAΔC were examined in HFFs infected with TRUS16HA-UL130V5 or with TRUS16HAΔC-UL130V5 (Fig. 7A). As expected, both proteins were detected starting from 48 h p.i. and remained detectable until 96 h p.i. The molecular mass of the pUS16HAΔC protein band, about 29 kDa, detected by the anti-HA MAb was smaller than that of pUS16HA (Fig. 7A) and fits well the predicted size of pUS16HAΔC (31 kDa), thus confirming the successful truncation of the C terminus of the US16 ORF. Next, we compared the growth kinetics of TRUS16HA-UL130V5, TRUS16HAΔC-UL130V5, and, as a control, TRΔUS16-UL130V5 in HMVECs and ARPE-19 cells. Replication of TRUS16HAΔC-UL130V5 in HFFs was similar to that of TRUS16HA-UL130V5 (data not shown). However, in both HMVECs and ARPE-19

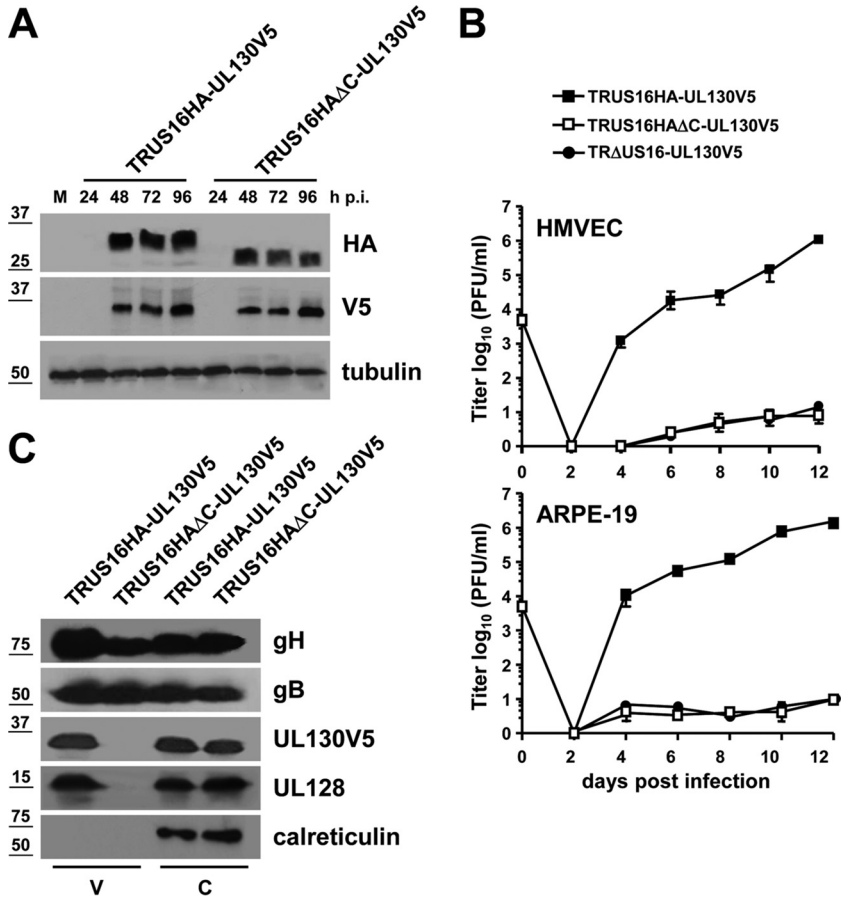

FIG 7 Truncation of the C-terminal tail of pUS16 impairs HCMV replication in endothelial and epithelial cells as well as incorporation of pentamer proteins into extracellular viral particles. (A) Kinetics of pUS16HA and pUS16HAΔC protein expression. HFFs were mock infected (lane M) or infected with TRUS16HA-UL130V5 or TRUS16HAΔC-UL130V5 (MOI of 1 PFU/cell), and at 24, 48, 72, and 96 h p.i. total protein cell extracts were prepared, fractionated by SDS-PAGE, and analyzed by immunoblotting with the anti-HA or anti-V5 MAb. The immunodetection of tubulin with an MAb was performed as an internal control. (B) TRUS16HAΔC-UL130V5 fails to replicate in endothelial and epithelial cells. HMVECs and ARPE-19 cells were infected with TRUS16HA-UL130V5, TRUS16HAΔC-UL130V5, or TRΔUS16-UL130V5 (MOI of 0.1 PFU/cell). The extent of virus replication was then assessed by titrating the infectivity of supernatants by plaque assay in HFFs. The data shown are the average of three experiments ± SD. (C) Effects of the C-terminal truncation of pUS16 on the levels of pentamer proteins incorporated into extracellular virions. TRUS16HA-UL130V5 and TRUS16HAΔC-UL130V5 extracellular virion particles were purified from culture supernatants of infected HFFs by centrifugation through 20% sorbitol cushions. Protein extracts prepared from virions (V) or infected cells (C) were then fractionated by SDS-PAGE and analyzed by immunoblotting with mouse MAb specific for gH, gB, UL128, or V5 to detect pUL130 protein. Immunodetection of calreticulin, as an endoplasmic reticulum marker, was performed as a control for cell protein contamination.

cells, TRUS16HAΔC-UL130V5 exhibited a severe growth defect similar to that observed for TRΔUS16-UL130V5 (Fig. 7B). Thus, deletion of the C-terminal tail of US16, as in TRUS16HAΔC-UL130V5, phenocopies the defective growth in endothelial and epithelial cells seen for US16-deficient viruses in which the whole US16 ORF was deleted or inactivated (Fig. 4) (12). Finally, immunoblot analysis of purified TRUS16HAΔC-UL130V5 virions produced by infected HFFs showed that deletion of the last C-terminal 34 amino acid residues of pUS16 reduced to undetectable levels the content of pUL128 and pUL130 in extracellular virus particles (Fig. 7C), as previously observed in genotypically negative US16 virions, such as those of TRΔUS16 (Fig. 3).

Altogether, these results point toward a role of the pUS16 C-terminal tail in causing the defective growth in endothelial and epithelial cells, as well as the specific alteration of the virion content of the pentamer already observed for US16-null mutant viruses.

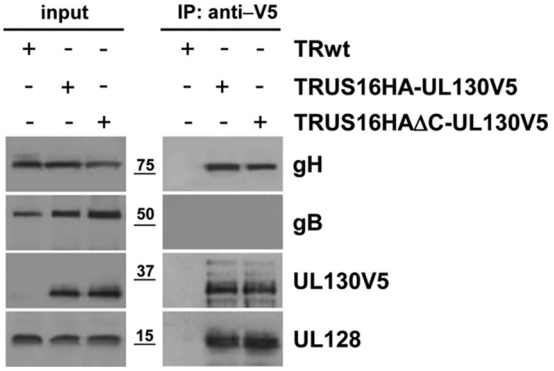

FIG 8 The C-terminal tail of the US16 protein is not required for the formation of the pentameric complex. HFF cells were infected with TRwt, TRUS16HA-UL130V5, or TRUS16HAΔC-UL130V5 (MOI of 1 PFU/cell). At 120 h p.i., cell extracts were prepared and immunoprecipitated using anti-V5 MAb. Then, immunoprecipitates and input cell extracts were analyzed by immunoblotting for detection of gH, gB, pUL128, and the V5 epitope.

The pUS16 C terminus is not required for assembly and trafficking of the pentamer. To investigate the impact of the deletion of the C-terminal segment of pUS16 on the pentamer pathway, we first analyzed formation of the pentameric complex in HFFs infected with TRUS16HA-UL130V5 or TRUS16HAΔC-UL130V5 by co-immunoprecipitation (co-IP). The data shown in Fig. 8 indicate that gH, pUL128, and pUL130V5 could be detected in anti-V5 immunoprecipitates from extracts of either TRUS16HA-UL130V5- or TRUS16HAΔC-UL130V5-infected HFFs, thus indicating that the absence of the C-terminal tail of pUS16 did not affect the assembly of the complex. The specificity of the co-IP assay was verified by the lack of detection of both the control gB, a viral glycoprotein not predicted to interact with UL130, and the pentamer proteins in V5 immunoprecipitates from the untagged TRwt infection (Fig. 8). Then, the subsequent stage of the pentamer complex maturation, namely, its trafficking from the ER, where it assembles (8), to the cVAC, was examined by immunofluorescence in cells infected with TRUS16HA-UL130V5 or TRUS16HAΔC-UL130V5. As shown in Fig. 9, in HFFs infected for 120 h, the pUS16HAΔC expressed by TRUS16HAΔC-UL130V5 (right panel) showed the same ring-like staining pattern as full-length pUS16 (left panel), demonstrating that the C-terminal deletion did not affect the trafficking of pUS16HAΔC to the cVAC. Similarly, the staining patterns of pUL130, gH, gB, and of tested cVAC markers (GM130, EEA1, and CD63) were akin to the patterns observed in TRUS16HA-UL130V5-infected cells (Fig. 9, left panel), thus indicating that deletion of the pUS16 C-terminal tail did not affect the trafficking of representative pentamer proteins to the cVAC or efficient cVAC formation. Moreover, immunolocalization of pUL130 and pUS16HAΔC showed the entirely overlapping ring-like, cytoplasmic staining pattern of the two proteins (Fig. 9, right panel), as already observed for the full-length pUS16HA (Fig. 9, left panel, and 5B).

Therefore, these results indicate that the C-terminal tail of pUS16 is not necessary for cVAC formation or the assembly and trafficking of the pentamer from the ER to the site of virus maturation and envelopment.

pUS16 and pUL130 interact in infected cells. The above results made it plausible that the link between the pUS16 and the pentamer might involve interactions between pUS16 and components of the complex. To investigate this hypothesis, co-IP assays were performed on protein extracts prepared from HFFs infected with TRUS16HA-UL130V5 or TRUS16HAΔC-UL130V5. As shown in Fig. 10A, we were able to detect gH, pUL130V5, pUL128, and gO but not pUS16HA in anti-gH immunoprecipitates of TRUS16HA-UL130V5-infected cells. However, we detected pUL130V5 and, as expected, pUS16HA but not gH, gO, and pUL128 in immunoprecipitates for HA (Fig. 10B). Reciprocally, pUS16HA along with gH and pUL128 was observed in immunoprecipitates for V5 from the same cell lysates that contained the tagged pUL130 (Fig. 10C). In

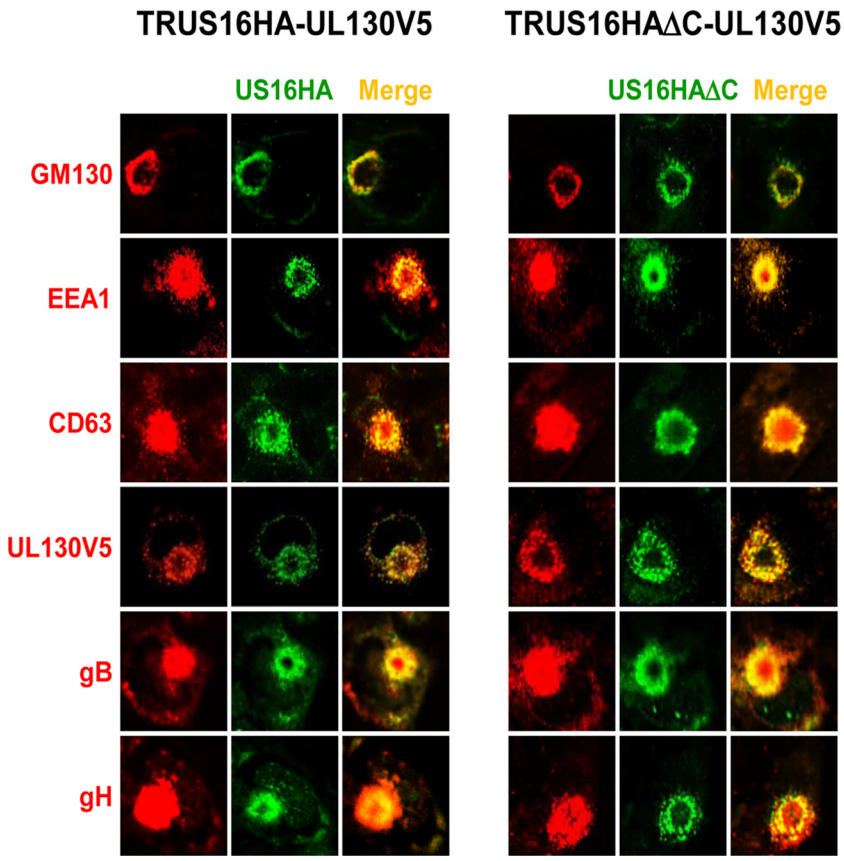

FIG 9 Lack of the C-terminal tail of pUS16 does not affect the trafficking of pentamer proteins to the cVAC of infected cells. HFF cells were infected with TRUS16HA-UL130V5 or TRUS16HAΔC-UL130V5 (MOI of 1 PFU/cell). At 120 h p.i., the cells were fixed, permeabilized, and stained green for pUS16HA and red for GM130, EEA1, CD63, V5, gB, or gH. Protein localization was visualized by confocal microscopy. Immunofluorescence experiments were repeated three times, and representative results are presented. Magnification, ×60.

contrast, we could not detect pUL130V5 in anti-HA immunoprecipitates from TRUS16HAΔC-UL130V5-infected cell extracts (Fig. 10D), suggesting that the C-terminal tail of pUS16 might be involved in the interaction with pUL130. Finally, lack of detection of proteins from control IgG IP as well as of the negative-control UL83 (Fig. 10, pp65) indicated that our anti-gH, anti-HA, and anti-V5 immunoprecipitates were specific for gH-, pUS16-, and pUL130-interacting proteins.

Taken together, these co-IP results suggest that pUS16, while not being able to directly interact with the mature pentamer complex or with gH/gL/gO, can associate with pUL130.

DISCUSSION

In a previous report, we observed that disruption of the US16 ORF in the genome of a low-passage-number HCMV strain impairs its ability to replicate in cell types that are major targets for productive lytic replication and dissemination in the natural host, such as endothelial and epithelial cells (12). In these cells, the replicative cycle of different US16-deficient viruses was blocked at a stage prior to the expression of IE genes; moreover, pUS16 could not be detected in purified virions produced from fibroblasts infected with US16-deficient viruses (12). However, this leaves open the question as to how pUS16 regulates certain pre-IE phases of the replication cycle in endothelial and epithelial cells even though it is not incorporated into virions released from producing cells.

Here, we provide evidence supporting the idea that the defective growth pheno-

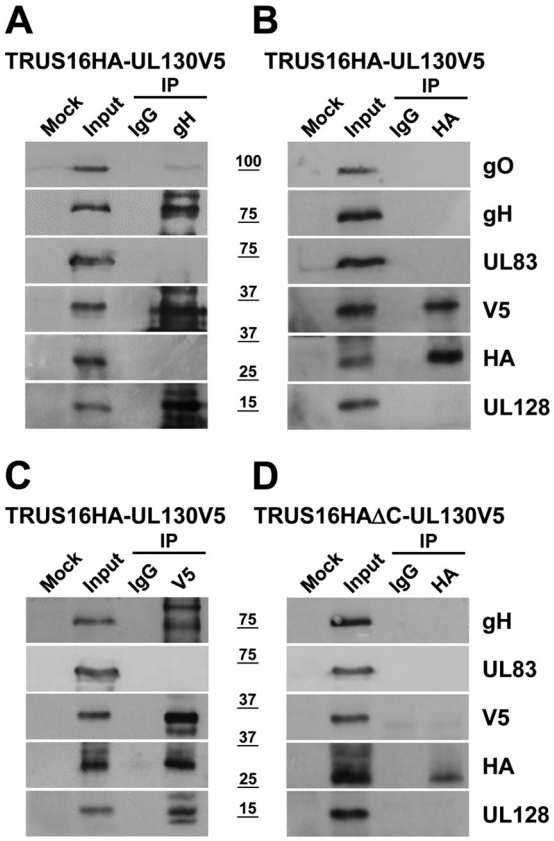

FIG 10 Interaction between pUS16 and pUL130 in infected cells. HFF cells were infected with TRUS16HA-UL130V5 or TRUS16HAΔC-UL130V5 (MOI of 1 PFU/cell). At 120 h p.i., cell extracts were prepared and immunoprecipitated using anti-gH (A), anti-HA (B, and D), and anti-V5 (C) MAbs or a nonspecific control IgG. Immunoprecipitates alongside input cell lysates were then analyzed by immunoblotting for detection of gO, gH, UL83 (pp65), pUL128, and the HA and V5 epitopes.

type of genotypically US16-negative virions in endothelial and epithelial cells is a consequence of deficiencies in the entry phase in these cell types. This failure has been related to a severe reduction of the pentamer content of extracellular viral particles produced in fibroblasts infected with US16-mutant viruses lacking either the whole US16 ORF or its C-terminal tail. However, in producer cells (i) the expression of representative pentamer proteins was not altered (Fig. 3 and 7), (ii) the pentameric complex was assembled correctly (Fig. 8), and (iii) the pentamer was normally transported to the cVAC (Fig. 9). Therefore, pUS16 seems to be dispensable for pentamer formation and trafficking to the site of secondary virus envelopment. Nonetheless, pUS16 was found to be required for the production of virus progeny with a high pentamer content. The lack of detectable interactions between pUS16 and the mature pentamer (Fig. 10), however, makes unlikely a direct action of pUS16 in the incorporation of the complex into virions. Currently, therefore, we can speculate that pUS16 would operate indirectly in the final maturation of endothelio- and epitheliotropic virus. The absence of pUS16 from extracellular viral particles (12), on the other hand, may support a role of pUS16 as an indirect producer-cell modifier of virion composition. Thus, in this scenario, pUS16 could promote interactions between not yet identified viral and/or cellular protein(s) and the mature pentamer that, in turn, mediate the efficient recruitment of pentamer-rich vesicles to tegumented nucleocapsids (3, 19). In-depth characterization of the protein-protein interactions that occur between pUS16 and other proteins in infected cells should prove helpful in sustaining or disproving this model.

Alternatively, one could speculate that pUS16 could prevent the retention in pro-

ducing cells of virus particles with a high pentamer content by interfering with the interaction between the pentamer and its specific cellular receptor. This would be consistent with the observation that genotypically US16-negative virions can efficiently infect other fibroblasts only due to the release of viral particles containing only gH/gL/gO. In this regard, it has been reported that fibroblasts infected with a low-passage-number HCMV release progeny composed of distinct endotheliotropic and nonendotheliotropic virus populations and that the endotheliotropic population has a high pentamer content (31). However, it is unlikely that the absence of pUS16 in producer cells affects the release of pentamer-rich virions because fibroblasts apparently do not express the receptor for the pentamer that is thought to be expressed in endothelial and epithelial cells (5–8) and that may be the molecule responsible for retaining the endotheliotropic HCMV population, as has been suggested in infected endothelial cells (31). Therefore, we may envisage that it is the lack of the specific incorporation of the pentamer into enveloped viruses, and not a defect in release of virions, that is responsible for the defective phenotype of US16-null viruses produced in fibroblasts.

Although an interaction of pUS16 with the pentamer was not observed, it was intriguing that there was an interaction between pUS16 and the pUL130 and that this interaction was prevented by the deletion of the C-terminal tail of pUS16 (Fig. 10), thus suggesting a possible involvement of this segment of pUS16 in binding pUL130. The absence of pUS16 in immunoprecipitates for gH from TRUS16HA-UL130V5-infected cells (Fig. 10A), on the other hand, suggests that pUS16 may bind a pUL130 surface that is sterically hindered in the assembled pentamer. The importance of the pUS16-pUL130 interaction for the incorporation of the pentamer, however, remains to be determined. In this regard, an interaction has been reported between pUL130 and the human Snapin protein, a component of the SNARE complex required for synaptic vesicle docking and exocytosis (32, 33), which may suggest a role of this interaction in pentamer incorporation and/or release of virions endowed with adequate amounts of the complex.

Another HCMV protein that regulates virus cell tropism by affecting the pentamer is UL148. In a recent study, it was reported that pUL148 modulates HCMV tropism by regulating the relative abundance of the two alternative gH/gL complexes on mature viral particles and that pUL148 exerts this effect during the assembly and/or maturation of the two complexes (34). pUL148 localizes to the ER and is not detected in the cVAC of HCMV-infected HFFs, while co-IP studies indicate interactions between pUL148 and several components of the two alternative gH/gL complexes during their assembly within the ER (34). In the proposed model, pUL148, by competing with pUL128 for loading onto immature gH/gL, selectively promotes the formation of the gH/gL/gO heterotrimer. Therefore, it was concluded that pUL148 impacts HCMV cell tropism by modulating the assembly of gH/gL complexes (35, 36). Here, we observed that pUS16 localizes to the cVAC, does not affect the assembly or the intracellular abundance of the pentameric complex, and does not physically interact with the mature pentamer. pUS16 thus influences the abundance of the pentamer in virions with a mechanism different from that exerted by UL148. Nevertheless, it is conceivable that both pUL148 and pUS16 contribute to shaping the final glycoprotein composition of the envelope of infectious virions by affecting the amounts and the incorporation of the pentamer, respectively, and in this way influencing the tropism of progeny virus.

Work from recent years from our and other laboratories supports the view that the US12 gene family encodes a series of regulatory proteins that impact different HCMV-host cell interactions. In fact, inactivation of some US12 gene members affects virus-mediated manipulation of the host innate immune response (37, 38) or, as we reported for US16 (12) and US20 (39), HCMV cell tropism. However, irrespective of the final outcome for virus-host cell interactions, the functions of several US12 proteins appear to be related to the late stages of HCMV maturation and the fine-tuning of the most appropriate protein composition of virions (38; this study). In this regard, identification of the luminal C-terminal tail of pUS16 as a domain required for HCMV's tropism for

TABLE 1 Oligonucleotides used for BAC mutagenesis

Primer designation	Sequence (5′ → 3′)
UL130_galk/kan_F	GCCTATACTATGTGTATGATGTCTCATAATAAAGCTCTCTTTCTCAGTCTCCTGTTGACAATTAATCATCG
UL130_galk/kan_R	GTTTTCAAAATTCCCTGCGCGCGCGACGGGCTCAAACGATGAGATTGGGACTCAGCAAAAGTTCGATTTA
UL130V5_F	GCCTATACTATGTGTATGATGTCT
UL130V5_R	GGTTTTCAAAATTCCCTGCGCGCGCGACGGGCCTACGTAGAATCAAGACCTAGGAGCGGGTTAGGGATTGGCTTACCAGCGCT AACGATGAGATTGGGAT
US16_galk/kan_F	CCCCACGGATCTCGCGCCTTAGACGCGCGGTCATATAGCCTCCGGCTGTCCCTGTTGACAATTAATCATCG
US16_galk/kan_R	CGTTCTCTGGAAACGGCTGCTCTGTCCGAAAACCAGTTCCGAACGAAAATCTCAGCAAAAGTTCGATTTA
US16HAΔC_F	CTAAAAGTCCCCCCACGGATCTCG
US16HAΔC_R1	CTAAGCGTAGTCTGGGACGTCGTATGGGTATCCTCCTCCCTGAAAATACAGGTTTTCTCCTCCGCTCAGCAGGTCCTGACAGTTGC
US16HAΔC_R2	CGTTCTCTGGAAACGGCTGCTCTGTCCGAAAACCAGTTCCGAACGAAAATCTAAGCGTAGTCTGGGACGTC

endothelial and epithelial cells supports the hypothesis that during the course of the evolution of the US12 gene family, an ancestral host-derived flexible structural protein scaffold associated with cellular membranes adapted to new purposes, fulfilling different and specific functions (13). In this model, changes occurring in the highly divergent N- and C-terminal amino acid sequences in the different US12 ORFs may have allowed the development of specific interactions with other cellular and/or viral proteins that, in turn, may regulate a broad range of specific activities within the infected cell. Further proteomics analyses by mass spectrometry of pUS16-containing protein complexes isolated from HCMV-infected cells may shed light on the global network of interactions occurring between pUS16 and other viral and/or cellular proteins and thus help to elucidate the details of the mechanism(s) through which pUS16 affects the acquisition of an envelope rich in the pentamer and thereby influences HCMV infectivity in clinically relevant cell types.

MATERIALS AND METHODS

Oligonucleotides. All oligonucleotides for PCR, mutagenesis, and sequencing were obtained from Life Technologies. Those used for BAC mutagenesis are listed in Table 1.

Bioinformatics. US16 topology was predicted using the Phyre, version 2.0, MEMSAT3, MEMSAT_SVM, TMHMM, version 2.0, and TopPred, version 0.01, programs. ClustalW, version 1.8, was used to identify amino acid sequence alignments.

Cells. Low-passage-number primary human foreskin fibroblasts (HFFs) were grown in Dulbecco's modified Eagle's medium (DMEM) (Biowest) supplemented with 10% fetal bovine serum (FBS) (Biowest). Human dermal microvascular endothelial cells (HMVECs) (CC-2543) were obtained from Clonetics and cultured as previously described (12). The retinal pigment epithelial cell line ARPE-19 (ATCC CRL-2302) was cultured in a 1:1 mixture of DMEM and Ham's F12 medium (Life Technologies) supplemented with 10% fetal calf serum (FCS).

Viruses. The HCMV laboratory strain AD169 was purchased from ATCC (VR538). The HCMV Towne bacterial artificial chromosome (BAC) (40) was a gift from Wolfram Brune. The wild-type TR BAC (NCBI accession no. AC146906.1) (41) was a gift from Jay Nelson. Reconstitution of the TR BAC in fibroblasts generated infectious virus that retained the ability to infect endothelial and epithelial cells (14).

Construction of TRΔUS16, TRUS16stop, and TRUS16HA mutants (Fig. 1) was described previously (12). The TRUS16HA-UL130V5 BAC (Fig. 1) was generated by a two-step replacement strategy using the *galK* recombineering method, as previously described (12, 39, 42, 43). Briefly, in the first step the *galK-kan* cassette was amplified out of the pGalK-Kan plasmid (a gift from Dong Yu) by PCR using the UL130_galK/kan primer set (Table 1). Specific sequences at the 3′ ends of the forward and reverse primers (21 and 20 bp, respectively) dictated the amplification of the *galK* cassette, and their 5′-end 50-bp tails were homologous to the sequences flanking the UL130-UL131 genes between nucleotides 213889 and 212641 of the complete TR BAC sequence. Following PCR, the PCR product was digested with DpnI to remove any plasmid template, gel purified, and then electroporated into SW102 bacteria harboring TRUS16HA BAC (12). The *galK-kan* cassette in TRUS16HA-ΔUL130 BAC was replaced in the second step with the UL130V5 cassette (amplified by PCR from the TR BAC using the UL130V5 primer set) (Table 1) that fused a sequence encoding a V5 epitope tag (GKPIPNPLLGLDST) to the C terminus of the UL130 ORF. Gal-negative colonies were characterized for replacement of the *galK-kan* sequences with the mutated UL130 version by PCR amplification of the whole segment, followed by restriction enzyme analysis and sequencing.

To generate the TRΔUS16-UL130V5 BAC (Fig. 1), the US16HA ORF in TRUS16HA-UL130V5 BAC was replaced with the *galK-kan* cassette amplified from pGalk-Kan using the US16_galK/kan primer set (Table 1).

The TRUS16HAΔC-UL130V5 BAC was derived from the TRΔUS16-UL130V5 BAC by replacing the *galK-kan* cassette with the US16HAΔC cassette (amplified by PCR from the TR BAC by the US16HAΔC primer set) (Table 1). In the US16HAΔC cassette, the HA epitope tag is fused in frame at the C terminus

of a truncated derivative of the US16 ORF in which the last 34 amino acids (from 276 to 309) have been deleted (Fig. 1).

Two independent TRUS16HA-UL130V5, TRΔUS16-UL130V5, and TRUS16HAΔC-UL130V5 BAC clones were selected and characterized to ensure that their phenotypes did not result from off-target mutations.

Infectious recombinant TRΔUS16, TRUS16stop, TRUS16HA-UL130V5, TRΔUS16-UL130V5, TRUS16HAΔC-UL130V5, TRwt, and Towne viruses were reconstituted in HFFs by transfection of the corresponding BAC DNA as previously described (12, 39). Viral titers were determined by plaque assay in HFFs.

Extracellular viral particles were concentrated from culture supernatants of HCMV-infected cells at 8 days p.i. by centrifugation at 6,000 × *g* for 1 h at 4°C and then partially purified through a 20% sorbitol cushion at 50,000 × *g* for 1 h at 4°C (12).

PEG-induced fusion. Treatment with polyethylene glycol (PEG) to stimulate the fusion between virion and cellular membranes was performed as previously described by Ryckman et al. (14). Briefly, ARPE-19 cells cultured in 24-well plates were infected with TRwt, AD169, Towne, TRUS16stop, or TRΔUS16 at an MOI of 0.1 PFU/cell, then immediately centrifuged at 2,000 rpm for 30 min, and incubated at 37°C for 2 h. Thereafter, cells were washed twice with warm phosphate-buffered saline (PBS), treated with 44% (vol/vol) PEG (Fluka) in PBS at 37°C for 60 s, and then washed immediately five times with warm PBS. After 24 h p.i., the number of IEA-positive cells was evaluated by immunofluorescence analysis.

Immunofluorescence. Immunofluorescence analysis was performed as previously described (12, 39) using the rat monoclonal antibody (MAb) anti-hemagglutinin (anti-HA) (clone 3F10; Roche) and mouse MAbs against V5 (clone R960-25; Life Technologies), IEA (IE1 plus IE2) (clone E13; Argene Biosoft), GM130 (clone 35/GM130; BD Biosciences), EEA1 (clone 14/EEA1; BD Biosciences), calreticulin (CALR) (clone 16/calreticulin; BD Biosciences), CD63 (sc-5275; Santa Cruz), gB (clone CH28; Virusys), gH (sc-58113; Santa Cruz), and UL83 (clone 3A12; Virusys). Selective permeabilization assays were performed as previously described (27).

The binding of primary antibodies was detected with CF594-conjugated rabbit anti-mouse IgG antibodies (Sigma) or with CF488A-conjugated rabbit anti-rat IgG (Sigma). Nuclei were counterstained with 4,6-diamidino-2-phenylindole (DAPI) where indicated in the legend to Fig. 2. Samples were then visualized with an Olympus IX50 fluorescence microscope equipped with Image-Pro Plus software. The intracellular localization of proteins was examined using an Olympus IX70 inverted laser scanning confocal microscope, and images were captured using FluoView 300 software (Olympus Biosystems). For quantitative colocalization of proteins, confocal microscopy images were analyzed to evaluate the Pearson's correlation coefficient by ImageJ as described by Adler and Parmryd (21).

Transmission electron microscopy. Prechilled HMVECs were infected with precooled purified TRwt or TRΔUS16 virus at an MOI of 30 PFU/cell at 4°C for 2 h. The cells were incubated at 37°C for 2 or 24 h and then processed for transmission electron microscopy. Infected cell pellets were fixed in a solution of 1.25% glutaraldehyde (Fluka, St. Louis, MO, USA), 1% paraformaldehyde (Merck, Darmstadt, Germany), and 0.5% sucrose in 0.1 M Sörensen phosphate buffer (pH 7.2) for 2 h at 4°C. Pellets were then washed in 0.1 M Sörensen phosphate buffer (pH 7.2) with 1.5% sucrose for 6 to 12 h, postfixed in 1 to 2% osmium tetroxide, dehydrated in ethanol, washed twice for 7 min with propylene oxide, and then embedded in Glauert's embedding mixture of resins, consisting of equal parts of araldite M and araldite Härter, plus HY 964 (Merck, Darmstadt, Germany), supplemented with 0.5% of the plasticizer dibutyl phthalate. Then, 2% of the accelerator DY 064 (Merck, Darmstadt, Germany) was added. Thin sections (70 nm) were cut using a Leica Ultracut UCT, stained with uranyl acetate and lead citrate, and examined with a JEM-1010 transmission electron microscope (JEOL, Tokyo, Japan) equipped with a MegaView III digital camera and a Soft Imaging System (SIS, Münster, Germany) for the computerized acquisition of images.

Immunoblotting and coimmunoprecipitation assay. For immunoblotting, the protein extractions, determination of protein concentrations, and immunoblot analysis were performed as previously described (12, 39). Immunostaining was carried out with a mouse MAb against V5 or with a rat anti-HA MAb conjugated to horseradish peroxidase (clone 3F10; Roche). Mouse MAbs against tubulin (clone TUB 2.1; Sigma), golgin-97 (sc-59820; Santa Cruz), and calreticulin (CALR) were used as controls for cellular protein loading. Immunostaining of proteins extracted from purified virions was carried out with mouse MAbs against V5, UL83, UL99 (clone CH19; Virusys), gB, and gH. Mouse MAbs against pUL128 (clone 4B10) and pUL130 (clone 3C5), were provided by Giuseppe Gerna. Immunocomplexes were detected with goat anti-mouse immunoglobulin antibodies conjugated to horseradish peroxidase (Life Technologies) and visualized by enhanced chemiluminescence (Western blotting Luminol reagent; Santa Cruz).

For coimmunoprecipitation, mock-infected and infected HFFs were lysed in Triton buffer (20 mM Tris-Cl, pH 6.8, 100 mM NaCl, 1% Triton X-100, 25 μl/ml protease inhibitor cocktail [P8340; Sigma]) and clarified by centrifugation at 16,000 × *g* (4°C for 30 min). Aliquots of 400 μg of protein were incubated at 4°C overnight with rotation with an anti-HA affinity matrix (clone 3F10), MAb against V5, mouse MAb against gH (clone 14-4B) (44, 45) (a gift from Bill Britt), or with control normal mouse IgG (Sigma); then immune complexes were collected using Protein A/G Plus agarose (Pierce). Beads were pelleted and washed three times with lysis buffer and boiled with Laemmli sample buffer, and supernatants were analyzed by immunoblotting with MAbs anti-V5, anti-HA, anti-gH (clone AP86) (46) (a gift from Bill Britt), anti-UL128, and anti-UL83 or with a rabbit polyclonal antipeptide antibody raised against HCMV TB40/e gO (47), kindly provided by Brent Ryckman.

Statistical analysis. All data are presented as means ± standard deviations (SD). The data were analyzed for significance using a paired *t* test and were considered statistically significant at a *P* value of ≤0.05. All statistical tests were performed using GraphPad Prism, version 5.01, for Windows (GraphPad Software).

ACKNOWLEDGMENTS

We gratefully thank Jay Nelson (Vaccine and Gene Therapy Institute, Oregon Health Science University), Wolfram Brune (Heinrich Pette Institute, Hamburg, Germany), Tom Shenk (Princeton University), Dong Yu (Washington University), Andrea Gallina (University of Milano), Giuseppe Gerna (IRCC Policlinico San Matteo, Pavia, Italy), Bill Britt (University of Alabama), and Brent Ryckman (University of Montana) for generously supplying reagents. We are grateful to Andrea Gallina for helpful discussions.

This work was supported by grants from the Italian Ministry for Universities and Scientific Research (PRIN 2010-11, grant no. 2010PHT9NF) to G.G. and from Ricerca Locale to A.L. and G.G.

REFERENCES

1. Britt W. 2008. Manifestations of human cytomegalovirus infection: proposed mechanisms of acute and chronic disease. Curr Top Microbiol Immunol 325:417–470.
2. Landolfo S, Gariglio M, Gribaudo G, Lembo D. 2003. The human cytomegalovirus. Pharmacol Therapeut 98:269–297. https://doi.org/10.1016/S0163-7258(03)00034-2.
3. Mocarski ES, Shenk T, Griffiths PD, Pass RF. 2013. Cytomegaloviruses, p 1960–2014. *In* Knipe DM, Howley PM, Cohen JI, Griffin DE, Lamb RA, Martin MA, Rancaniello VR, Roizman B (ed), Fields virology, 6th ed, vol 2. Lippincott Williams & Wilkins, Philadelphia, PA.
4. Goodrum F, Caviness K, Zagallo P. 2012. Human cytomegalovirus persistence. Cell Microbiol 14:644–655. https://doi.org/10.1111/j.1462-5822.2012.01774.x.
5. Sinzger C, Digel M, Jahn G. 2008. Cytomegalovirus cell tropism. Curr Top Microbiol Immunol 325:63–83.
6. Revello MG, Gerna G. 2010. Human cytomegalovirus tropism for endothelial/epithelial cells: scientific background and clinical implications. Rev Med Virol 20:136–155. https://doi.org/10.1002/rmv.645.
7. Vanarsdall AL, Johnson DC. 2012. Human cytomegalovirus entry into cells. Curr Opin Virol 2:37–42. https://doi.org/10.1016/j.coviro.2012.01.001.
8. Ryckman BJ, Rainish BL, Chase MC, Borton JA, Nelson JA, Jarvis MA, Johnson DC. 2008. Characterization of the human cytomegalovirus gH/gL/UL128-131 complex that mediates entry into epithelial and endothelial cells. J Virol 82:60–70. https://doi.org/10.1128/JVI.01910-07.
9. Dunn W, Chou C, Li H, Hai R, Patterson D, Stolc V, Zhu H, Liu F. 2003. Functional profiling of a human cytomegalovirus genome. Proc Natl Acad Sci U S A 100:14223–14228. https://doi.org/10.1073/pnas.2334032100.
10. Yu D, Silva MC, Shenk T. 2003. Functional map of human cytomegalovirus AD169 defined by global mutational analysis. Proc Natl Acad Sci U S A 100:12396–12401. https://doi.org/10.1073/pnas.1635160100.
11. Murphy E, Shenk T. 2008. Human cytomegalovirus genome. Curr Top Microbiol Immunol 325:1–19.
12. Bronzini M, Luganini A, Dell'Oste V, De Andrea M, Landolfo S, Gribaudo G. 2012. The US16 gene of human cytomegalovirus is required for efficient viral infection of endothelial and epithelial cells. J Virol 86:6875–6888. https://doi.org/10.1128/JVI.06310-11.
13. Lesniewski M, Das S, Skomorovska-Prokvolit Y, Wang FZ, Pellet PE. 2006. Primate cytomegalovirus US12 gene family: a distinct and diverse clade of seven-transmembrane proteins. Virology 354:286–298. https://doi.org/10.1016/j.virol.2006.06.035.
14. Ryckman BJ, Jarvis MA, Drummond DD, Nelson JA, Johnson DC. 2006. Human cytomegalovirus entry into epithelial and endothelial cells depends on genes UL128 to UL150 and occurs by endocytosis and low-pH fusion. J Virol 80:710–722. https://doi.org/10.1128/JVI.80.2.710-722.2006.
15. Vanarsdall AL, Wisner TW, Lei H, Kazlauskas A, Johnson DC. 2012. PDGF receptor-α does not promote HCMV entry into epithelial and endothelial cells but increased quantities stimulate entry by an abnormal pathway. PLoS Pathog 8:e1002905. https://doi.org/10.1371/journal.ppat.1002905.
16. Das S, Pellet PE. 2007. Members of the HCMV US12 family of predicted heptaspanning membrane proteins have unique intracellular distributions, including association with the cytoplasmic virion assembly complex. Virology 361:263–273. https://doi.org/10.1016/j.virol.2006.11.019.
17. Das S, Vasanji A, Pellet PE. 2007. Three-dimensional structure of the human cytomegalovirus virion assembly complex includes a reoriented secretory apparatus. J Virol 81:11861–11869. https://doi.org/10.1128/JVI.01077-07.
18. Das S, Pellet PE. 2011. Spatial relationships between markers for secretory and endosomal machinery in human cytomegalovirus-infected cells versus those in uninfected cells. J Virol 85:5864–5879. https://doi.org/10.1128/JVI.00155-11.
19. Tandon R, Mocarski ES. 2012. Viral and host control of cytomegalovirus maturation. Trends Microbiol 20:392–401. https://doi.org/10.1016/j.tim.2012.04.008.
20. Alwine JC. 2012. The human cytomegalovirus assembly compartment: a masterpiece of viral manipulation of cellular processes that facilitates assembly and egress. PLoS Pathog 8:e1002878. https://doi.org/10.1371/journal.ppat.1002878.
21. Adler J, Parmryd I. 2013. Colocalization analysis in fluorescence microscopy. Methods Mol Biol 931:97–109. https://doi.org/10.1007/978-1-62703-056-4_5.
22. Patrone M, Secchi M, Fiorina L, Ierardi M, Milanesi G, Gallina A. 2005. Human cytomegalovirus UL130 protein promotes endothelial cell infection through a producer cell modification of the virion. J Virol 79:8361–8373. https://doi.org/10.1128/JVI.79.13.8361-8373.2005.
23. Kelley LA, Mezulis S, Yates CM, Wass MN, Sternberg MJE. 2015. The Phyre2 web portal for protein modeling, prediction and analysis. Nat Protoc 10:845–858. https://doi.org/10.1038/nprot.2015.053.
24. Nugent T, Jones D. 2009. Transmembrane protein topology prediction using support vector machines. BMC Bioinformatics 10:159. https://doi.org/10.1186/1471-2105-10-159.
25. Claros MG, von Heijne G. 1994. TopPred II: an improved software for membrane protein structure predictions. Comput Appl Biosci 10:685–686.
26. Krogh A, Larsson B, von Heijne G, Sonnhammer EL. 2001. Predicting transmembrane protein topology with a hidden Markov model: application to complete genomes. J Mol Biol 305:567–580. https://doi.org/10.1006/jmbi.2000.4315.
27. Carrara G, Saraiva N, Gubser C, Johnson BF, Smith GL. 2012. Six-transmembrane topology for Golgi anti-apoptotic protein (GAAP) and Bax inhibitor 1 (BI-1) provides model for the transmembrane Bax inhibitor-containing motif (TMBIM) family. J Biol Chem 287:15896–15905. https://doi.org/10.1074/jbc.M111.336149.
28. Nakamura N, Rabouille C, Watson R, Nilsson T, Hui N, Slusarewicz P, Kreis TE, Warren G. 1995. Characterization of a *cis*-Golgi matrix protein, GM130. J Cell Biol 131:1715–1726. https://doi.org/10.1083/jcb.131.6.1715.
29. Bedard K, Szabo E, Michalak M, Opas M. 2005. Cellular functions of endoplasmic reticulum chaperones calreticulin, calnexin, and ERp57. Int Rev Cytol 245:91–121. https://doi.org/10.1016/S0074-7696(05)45004-4.
30. Sanchez V, Greis KD, Sztul E, Britt WJ. 2000. Accumulation of virion tegument and envelope proteins in a stable cytoplasmic compartment during human cytomegalovirus replication: characterization of a potential site of virus assembly. J Virol 74:975–986. https://doi.org/10.1128/JVI.74.2.975-986.2000.
31. Scrivano L, Singzer C, Nitschko H, Koszinowski UH, Adler B. 2011. HCMV spread and cell tropism are determined by distinct virus populations. PLoS Pathog 7:e1001256. https://doi.org/10.1371/journal.ppat.1001256.
32. Wang G, Ren G, cui X, Lu Z, Ma Y, Qi Y, Huang Y, Liu Z, Sun Z, Ruan Q. 2016. Host protein Snapin interacts with human cytomegalovirus pUL130 and affects viral DNA replication. J Biosci 41:173–182. https://doi.org/10.1007/s12038-016-9604-2.
33. Kasai H, Takahashi N, Tokumaru H. 2012. Distinct initial SNARE configu-

rations underlying the diversity of exocytosis. Physiol Rev 92:1915–1964. https://doi.org/10.1152/physrev.00007.2012.
34. Li G, Nguyen CC, Ryckman BJ, Britt W, Kamil JP. 2015. A viral regulator of glycoprotein complexes contributes to human cytomegalovirus cell tropism. Proc Natl Acad Sci U S A 112:4471–4476. https://doi.org/10.1073/pnas.1419875112.
35. Li G, Kamil JP. 2015. Viral regulation of cell tropism in human cytomegalovirus. J Virol 90:626–629. https://doi.org/10.1128/JVI.01500-15.
36. Adler B. 2015. A viral pilot for HCMV navigation? Viruses 7:3857–3862. https://doi.org/10.3390/v7072801.
37. Fielding CA, Aicheler R, Stanton RJ, Wang ECY, Han S, Seirafian S, Davies J, McSharry BP, Weekes MP, Antrobus PR, Prod'homme V, Blanchet FP, Sugrue D, Cuff S, Roberts D, Davison AJ, Lehner PJ, Wilkinson GWG, Tomasec P. 2014. Two novel human cytomegalovirus NK cell evasion functions target MICA for lysosomal degradation. PLoS Pathog 10:e1004058. https://doi.org/10.1371/journal.ppat.1004058.
38. Gurczynski S, Das S, Pellet PE. 2014. Deletion of the human cytomegalovirus US17 gene increases the ratio of genomes per infectious unit and alters regulation of immune and endoplasmic reticulum stress response genes at early and late times after infection. J Virol 88:2168–2182. https://doi.org/10.1128/JVI.02704-13.
39. Cavaletto N, Luganini A, Gribaudo G. 2015. Inactivation of the Human cytomegalovirus US20 gene hampers productive viral replication in endothelial cells. J Virol 89:11092–11106. https://doi.org/10.1128/JVI.01141-15.
40. Marchini A, Liu H, Zhu H. 2001. Human cytomegalovirus with IE-2 (UL122) deleted fails to express early lytic genes. J Virol 75:1870–1878. https://doi.org/10.1128/JVI.75.4.1870-1878.2001.
41. Murphy E, Yu D, Grimwood J, Schmutz J, Dickson M, Jarvis MA, Hahn G, Nelson JA, Myers RM, Shenk T. 2003. Coding potential of laboratory and clinical strains of human cytomegalovirus. Proc Natl Acad Sci U S A 100:14976–14981. https://doi.org/10.1073/pnas.2136652100.
42. Warming S, Costantino N, Court DL, Jenkins NA, Copeland NG. 2005. Simple and highly efficient BAC recombineering using *galK* selection. Nucleic Acids Res 33:e36. https://doi.org/10.1093/nar/gni035.
43. Caposio P, Luganini A, Bronzini M, Landolfo S, Gribaudo G. 2010. The Elk-1 and serum response factor binding sites in the major immediate-early promoter of human cytomegalovirus are required for efficient viral replication in quiescent cells and compensate for inactivation of the NF-κB sites in proliferating cells. J Virol 84:4481–4493. https://doi.org/10.1128/JVI.02141-09.
44. Britt WJ, Vugler L, Butfiloski EJ, Stephens EB. 1990. Cell surface expression of human cytomegalovirus (HCMV) gp55-116 (gB): use of HCMV-recombinant vaccinia virus-infected cells in analysis of the human neutralizing antibody response. J Virol 64:1079–1085.
45. Bogner E, Reschke M, Reis B, Reis E, Britt W, Radsak K. 1992. Recognition of compartmentalized intracellular analogs of glycoprotein H of human cytomegalovirus. Arch Virol 126:67–80. https://doi.org/10.1007/BF01309685.
46. Urban M, Britt W, Mach M. 1992. The dominant linear neutralizing antibody-binding site of glycoprotein gp86 of human cytomegalovirus is strain specific. J Virol 66:1303–1311.
47. Zhou M, Yu Q, Wechsler A, Ryckman BJ. 2013. Comparative analysis of gO isoforms reveals that strains of human cytomegalovirus differ in the ratio of gH/gL/gO and gH/gL/UL128-131 in the virion envelope. J Virol 87:9680–9690. https://doi.org/10.1128/JVI.01167-13.